

Equilibrium and Dynamics of Multispecies Nonneutral Plasmas with a Single Sign of Charge

Daniel H. E. Dubin

Department of Physics, University of California at San Diego, La Jolla, CA USA 92093-0319

Abstract. The phenomenon of centrifugal separation in a rotating multispecies plasma column is discussed. Rate equations for collisional separation are derived. Two electrostatic instabilities that are driven by centrifugal effects are also considered: a diocotron mode and a drift wave.

Keywords: nonneutral plasma, diocotron modes, drift waves, transport

PACS: 52.27.Jt, 52.35.-g, 52.35.Fp, 52.25.Fi

Many experiments on nonneutral plasmas involve multiple plasma species. Some experiments deliberately mix species in order to apply techniques such as sympathetic cooling, where one species is cooled (or otherwise manipulated) through its interactions with another cold species [1, 2, 3]. However, even experiments on “single species” plasmas often have contaminants. For instance, “pure” ion plasmas can contain isotopes of a given species [4]; and charge exchange or other chemical reactions with neutral background gas also often lead to increased contamination over time [5]. Even pure electron plasmas can be contaminated by negative ions (e.g. H^-) [6].

These multispecies nonneutral plasmas have several characteristics not shown by single species plasmas. For instance, they exhibit collective waves such as ion sound waves, drift waves and ITG waves that do not occur in single species plasmas [7]. Here we consider the phenomenon of centrifugal separation, which requires species with different masses, considering several mechanisms by which this separation can occur. For simplicity we focus on cases where all species have the same charge q .

EQUILIBRIUM PROFILES

Nonneutral plasmas magnetically confined in Penning-Malmberg traps rotate about their axis of symmetry, and this rotation produces a centrifugal separation of plasma species with heavier species pushed to the outside of the plasma. The degree of separation depends on plasma temperature T and rotation frequency ω_r . Assuming that the plasma is in thermal equilibrium (uniform T and rigid rotation at frequency ω_r for all species), the density of two species a and b are in the ratio given by the Boltzmann factor

$$\frac{n_a(r)}{n_b(r)} = C_{ab} \exp \left[\frac{1}{2T} (m_a - m_b) \omega_r^2 r^2 \right] \quad (1)$$

where m_a and m_b are particle mass for each species, r is cylindrical radius, and C_{ab} is a constant determined by the overall concentration of each species. Separation requires

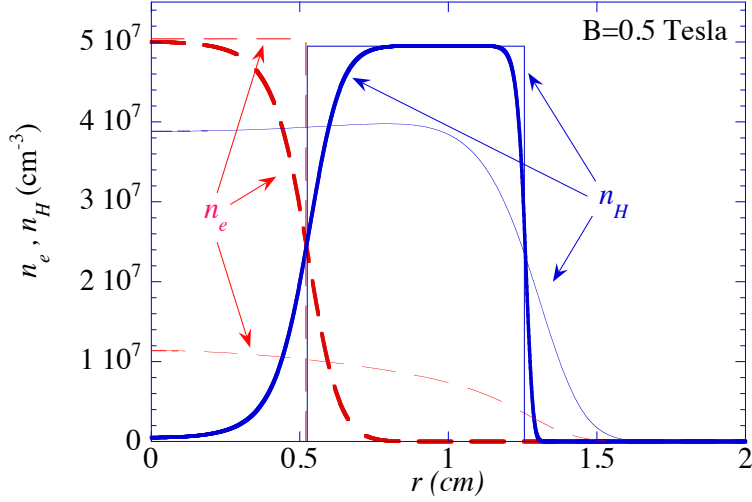


FIGURE 1. Electron and H^- densities (dashed and solid lines respectively) versus radius in a thermal equilibrium at three temperatures: $T = 0$, $T = 300$ K and $T = 1$ eV. At $T = 0$ the species are completely separated, while at $T = 1$ eV they are mixed. In all cases $B = 0.5$ Tesla.

that the magnitude of the exponent be greater than unity at a radius r within the plasma, which implies

$$\omega_r r > \sqrt{2T/|m_a - m_b|}. \quad (2)$$

This inequality can also be written in terms of total plasma density $n_0 = \sum_a n_a$, if we assume a low temperature plasma whose radius is much larger than the Debye length, so that total density within the plasma is nearly uniform. If we further assume that the plasma density is well below the Brillouin limit for all species, then rotation is due mostly to the $E \times B$ drift [8],

$$\omega_r \approx \frac{2\pi q c n_0}{B}, \quad (3)$$

and then Eq. (2) can be written as

$$n_0 r > 7 \times 10^5 \text{ cm}^{-2} B(\text{Tesla}) \sqrt{\frac{T(K)}{|m_a - m_b|(\text{amu})}}. \quad (4)$$

For instance, a room temperature e^-H^- plasma in a 1 Tesla magnetic field with radius $r_p = 1$ cm requires a total density greater than roughly 10^7 cm^{-3} to exhibit significant centrifugal separation. Example density profiles are exhibited in Fig. 1 for three temperatures. All three cases have the same particle number and total angular momentum. At the lowest temperature there is complete separation between species, with a small vacuum gap Δr between species given by [9]

$$\frac{\Delta r}{r_p} \left(2 + \frac{\Delta r}{r_1}\right) = \omega_r \frac{(m_H - m_e)c}{eB}, \quad (5)$$

where r_1 is the radius of the (inner) electron column. In this example the gap is only 0.005 cm. At higher temperature the species interpenetrate in such a way that Eq. (1) is satisfied but the total density n_0 is nearly uniform within the plasma. This is because when $\omega_r(m_b - m_a)c/qB \ll 1$, radial electrostatic force dominates over the centrifugal force, so total charge density, determined mainly by electrostatic and magnetic force balance, is largely unaffected by the weak centrifugal effects. Thus each species density is in ratio given by Eq. (1), but the total density is nearly uniform.

COLLISIONAL SEPARATION STATES

Centrifugal separation is driven by various processes, for instance, collisions between species. The following fluid analysis provides rate equations for collisional centrifugal separation.

For a plasma column that has not yet come to thermal equilibrium, the fluid rotation frequency ω_{r_a} for each species (labeled a) can differ from one another, as determined by radial force balance:

$$0 = n_a \left[qE(r) + \frac{qB}{c} \omega_{r_a} r + m_a \omega_{r_a}^2 r \right] - \frac{\partial p_a}{\partial r} \quad (6)$$

where $E(r)$ is the radial electric field and $p_a = n_a T_a$ is the pressure for species a . This can be solved for ω_{r_a} . It is convenient to write the solution as

$$\omega_{r_a} = \omega_E(r) + \frac{c}{qB n_a(r) r} \frac{\partial p_a}{\partial r} - \frac{\omega_{r_a}^2}{\Omega_{c_a}}, \quad (7)$$

where $\omega_E(r) = -E(r)c/Br$ is the $E \times B$ drift frequency, and $\Omega_{c_a} = qB/m_a c$ is the cyclotron frequency of species a . The last term is the centrifugal correction to the rotation rate, assumed small.

Since each species generally rotates at a different rate, there is a collisional drag between species that causes the separation. Here we assume a simple drag force on species a of the form

$$F_{\text{drag } a} = - \sum_b v_{ab} m_a r (\omega_{r_a} - \omega_{r_b}) \quad (8)$$

where v_{ab} is the frequency of collisions between species a and b . The form of this drag force can be verified, and an expression for v_{ab} can be derived, from kinetic theory [10]. In turn, this drag force (in the θ direction) produces an $F \times B$ drift in the radial direction that causes centrifugal separation. Using Eqs. (7) and (8), the radial particle flux Γ_{r_a} of species a is

$$\begin{aligned} \Gamma_{r_a} &= n_a \frac{c F_{\text{drag } a}}{qB} \\ &= - \sum_b \frac{D_{ab}}{T_a} \left[\frac{\partial p_a}{\partial r} - \frac{n_a}{n_b} \frac{\partial p_b}{\partial r} + n_a (m_b \omega_{r_b}^2 - m_a \omega_{r_a}^2) r \right] \end{aligned} \quad (9)$$

where $D_{ab} = v_{ab} r_{ca}^2$ is a diffusion coefficient and $r_{ca} = \sqrt{T_a/m_a}/\Omega_{ca}$ is the thermal cyclotron radius for species a . The first two terms in Eq. (9) are diffusive fluxes, and the last is a mobility flux due to the centrifugal force acting on each species.

Note that this flux vanishes when $T_a(r) = T_b(r) = T$, $\omega_{r_a}(r) = \omega_{r_b}(r) = \omega_r$ and the species densities are in ratio given by Eq. (1) (i.e., they are in thermal equilibrium). It can further be shown that the flux given by Eq. (9) drives the system toward this thermal equilibrium state, since it causes a monotonic increase in entropy [11]. However, the flux described by Eq. (9) leaves the total density unaffected, because the total flux $\sum_a \Gamma_{r_a}$ vanishes. This can be seen by writing the total flux as

$$\begin{aligned} \sum_a \Gamma_{r_a} &= - \left(\frac{c}{qB} \right)^2 \sum_{a,b} m_a n_a v_{ab} \left[\frac{1}{n_a} \frac{\partial p_a}{\partial r} - \frac{1}{n_b} \frac{\partial p_b}{\partial r} + (m_b \omega_{r_b}^2 - m_a \omega_{r_a}^2) r \right] \\ &= 0. \end{aligned} \quad (10)$$

(Momentum conservation implies that $m_a n_a v_{ab} = m_b n_b v_{ba}$, so the sum is antisymmetric under interchange of species labels and hence vanishes.) Evolution of total density requires extra fluxes not included in Eq. (9), such as viscous flux due to shears in the rotation frequency. However, total density need not change by very much during centrifugal separation, if $\frac{\omega_r(m_b - m_a)c}{qB} \ll 1$. For example, for the density profiles shown in Fig. 1, total density is almost the same in each case (with the largest variation in n_0 occurring at the species edges).

The rate \mathcal{R} of centrifugal separation implied by Eq. (9) can be estimated, assuming that mobility is on the same order, or less than, the diffusive flux. This rate is then roughly the rate required for particles to diffuse across the plasma radius r_p ,

$$\mathcal{R} \sim \frac{D_{ab}}{r_p^2} \sim 0.1 s^{-1} \left(\frac{n_0}{10^7 \text{cm}^{-3}} \right) \sqrt{\frac{\mu(\text{amu})}{T(\text{K})}} \frac{1}{(B(\text{Tesla})r_p(\text{cm}))^2} \quad (11)$$

where we have estimated the diffusion coefficient using Ref. [11], and where μ is the reduced mass for the two plasma species. This rate is typically slow compared to many other plasma timescales, so it is worth considering whether processes other than collisions can lead to centrifugal separation.

DIOCOTRON INSTABILITY

We therefore turn to collective plasma instabilities that can be driven by centrifugal forces. In neutral plasma confinement such instabilities play an important role, as they are related to the well-known interchange instabilities that grow on MHD timescales. Here we consider purely electrostatic instabilities in keeping with the typical low density (low “beta”) of nonneutral plasmas.

We first consider the diocotron mode in a multispecies nonneutral plasma column, showing that it can be driven unstable by centrifugal effects under certain conditions. The diocotron mode is a 2-D disturbance [in the $(r - \theta)$ plane] of the plasma density and potential, propagated by drift motion. In the low-density regime ($\omega_r/\Omega_{ca} \ll 1$ for

all species), it is well-described by the following 2-D linearized continuity equation for each species,

$$\frac{\partial \delta n_a}{\partial t} + \omega_{r_a} \frac{\partial \delta n_a}{\partial \theta} + \delta v_r \frac{\partial n_a}{\partial r} = 0, \quad (12)$$

where $\delta n_a(r, \theta, t)$ is the perturbed density, $n_a(r)$ is the equilibrium density profile, $\omega_{r_a}(r)$ is the equilibrium drift rotation frequency given approximately by

$$\omega_{r_a} = \omega_E - \frac{\omega_{r_a}^2}{\Omega_{c_a}}, \quad (13)$$

and δv_r is the perturbed radial fluid velocity. We assume that this velocity is well-described by $E \times B$ drift dynamics (this can be verified by a more detailed analysis in the low density regime [7]), writing

$$\delta v_r = -\frac{c}{Br} \frac{\partial \delta \phi}{\partial \theta}, \quad (14)$$

where $\delta \phi(r, \theta, t)$ is the perturbed electrostatic potential. The system of differential equations is closed by the Poisson equation,

$$\nabla^2 \delta \phi = -4\pi q \sum_a \delta n_a. \quad (15)$$

Fourier analyzing in θ and t , we assume perturbed quantities vary as $e^{i\omega t + i\ell\theta}$. Equations (12) and (14) can then be combined to yield

$$\delta n_a = \frac{\ell c}{Br} \delta \phi \frac{\partial n_a / \partial r}{\ell \omega_{r_a} - \omega}. \quad (16)$$

A dispersion relation for ω is then obtained by substituting Eq. (16) into Eq. (15):

$$\nabla^2 \delta \phi = -\frac{4\pi q \ell c}{Br} \delta \phi \sum_a \frac{\partial n_a / \partial r}{\ell \omega_{r_a} - \omega}. \quad (17)$$

This equation can be solved for ω and $\delta \phi(r)$, with the homogeneous boundary condition that $\delta \phi = 0$ at the conducting wall radius r_w . The usual diocotron mode dispersion relation is obtained by substituting $\omega_{r_a} = \omega_E$, in which case Eq. (17) depends on n_a only through the sum $n_0 = \sum_a n_a$; all species have identical $E \times B$ dynamics when centrifugal effects are neglected. However, when centrifugal effects are added via Eq. (13), new modes appear near the $E \times B$ rotation frequency $\ell \omega_E$. For the case of the zero temperature density profiles shown in Fig. 1, a standard analysis shows that the new modes have frequencies given, to lowest order in $\omega_E(m_2 - m_1)c/qB$, by the expression

$$\omega = \ell \omega_E \pm \sqrt{\left| \frac{\ell \omega_E^2}{qB} \right| c(m_2 - m_1)(1 - r_1^{2\ell}/r_p^{2\ell}) \left(1 + O\left(\frac{\omega_E(m_2 - m_1)c}{B} \right) \right)}. \quad (18)$$

Here, the small gap between species is neglected, r_1 is the inner radius separating species with species 1 in the region $0 < r < r_1$, and r_p is the outer plasma radius with species 2 in the region $r_1 < r < r_p$.

These modes are self shielded, producing no potential perturbation outside the plasma, and are unstable if $m_2 < m_1$, that is, if the heavy species resides on the *inside* of the plasma column. The instability has been observed in particle-in-cell simulations, to be described in a separate publication. The resulting turbulent flow tends to mix the species but does not separate the heavy species on the outer plasma edge at low temperature, as would be expected in thermal equilibrium. This is not surprising since there is no temperature dependence in the diocotron dynamics, so there is no way for this instability to discriminate between low temperatures that lead to separation and high temperatures that do not.

DRIFT-WAVE INSTABILITY

However, there are other temperature-dependent modes that can be driven unstable by centrifugal effects. These are the well-known drift waves, of great importance to neutral plasma confinement. In a multispecies nonneutral plasma it has been shown that these waves can also occur under circumstances where one species (labeled species 1) behaves adiabatically in the potential perturbation

$$\delta n_1 \simeq -\frac{q\delta\phi}{T_1} n_1 (1 + i\beta) \quad (19)$$

(where β is the nonadiabatic correction, assumed small) while the other species (labeled 2) behaves nonadiabatically, as a 2-D fluid with density perturbations given by Eq. (16). As discussed in Ref. [7], the mode is approximately described by a dispersion relation of the form

$$\nabla^2 \delta\phi = \frac{\delta\phi(1 + i\beta)}{\lambda_{D1}^2} + \frac{4\pi\ell qc}{Br} \delta\phi \frac{\partial n_2 / \partial r}{\omega - \ell\omega_{r2}} \quad (20)$$

where $\lambda_{D1}^2 = T_1 / 4\pi q^2 n_1$. The first term on the right describes a Debye-shielding response by the adiabatic species, and the second term is the same 2-D drift response as for diocotron modes. These responses require that

$$\omega - \ell\omega_{r1} \ll k_z \bar{v}_1, \quad \text{and} \quad \omega - \ell\omega_{r2} \gtrsim 4k_z \bar{v}_2, \quad (21)$$

where k_z is the parallel wave number of the mode, and \bar{v}_a is the thermal speed of species a .

A local dispersion relation can be obtained by replacing ∇^2 by $-k^2$, which yields

$$\omega - \ell\omega_{r2} = \frac{\ell\omega_*}{(1 + i\beta)} \quad (22)$$

where

$$\omega_* = \frac{T_1 c}{Br n_1} \frac{\partial n_2}{\partial r} / (1 + \lambda_{D1}^2 k^2). \quad (23)$$

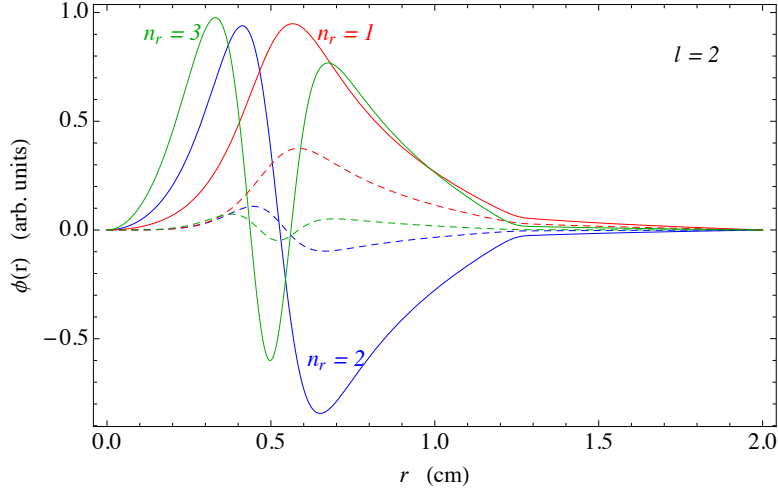


FIGURE 2. Three unstable drift wave eigenmodes for the plasma densities shown in Fig. 1 (with thick lines), taking $T = 1$ eV and $B = 0.5T$, for $\ell = 2$ and $n_r = 1, 2$, and 3 . Modes are found by solving Eq. (26). Dashed lines are the imaginary part and solid lines are the real part.

Applying this local dispersion relation to the requirements (21) for a drift-wave yields

$$\frac{r_{c1}}{rn_1} \frac{\partial n_2}{\partial r} \ll \frac{k_z}{\ell} \lesssim 4 \frac{r_{c2}}{rn_1} \frac{\partial n_2}{\partial r} \quad (24)$$

where we assumed $k\lambda_D < 1$. It is possible to satisfy these inequalities provided the mass ratio m_1/m_2 is sufficiently small and ℓ is sufficiently large (but $k\lambda_{D1} < 1$). Taking $\ell \lesssim r/\lambda_{D1}$ and $T_1 = T_2 = T$, the right inequality becomes

$$k_z \lesssim 4 \frac{r_{c2}}{\lambda_{D1} n_1} \frac{\partial n_2}{\partial r} = 4 \frac{\omega_{p2}}{\Omega_{c2} \sqrt{n_1 n_2}} \frac{\partial n_2}{\partial r}, \quad (25)$$

implying that the plasma column must be fairly long when $\omega_{p2}/\Omega_{c2} \ll 1$.

An example where these requirements are satisfied is shown by the $T = 300\text{K}$ profiles in Fig. 1. The density profiles of the electron- H^- plasma are thermal equilibrium profiles when $T = 300\text{K}$, but if the temperature is raised to $T = 1\text{eV}$ these profiles become drift-wave unstable. A solution of Eq. (20) in a 100 cm long plasma with a conducting boundary at a radius of 2cm, yields a series of unstable modes for different ℓ numbers, a few of which are displayed in Fig. 2. The real part of the frequencies and the growth rates for some of the modes are shown in Fig. 3. In these calculations β is taken to be given by the expression for collisionless guiding-center motion [7],

$$\beta = \sqrt{\frac{\pi}{2} \frac{\omega - \ell(\omega_E + \omega_{D1})}{k_z^2 \bar{v}_1}} \quad (26)$$

where $\omega_{D1} = \frac{Tc}{qBn_1 r} \frac{\partial n_1}{\partial r}$ is the diamagnetic drift frequency of species 1 (the nearly adiabatic species).

These unstable modes would be expected to rapidly saturate and produce transport that leads to mixing of the ions and electrons, driving the plasma toward the mixed 1 eV

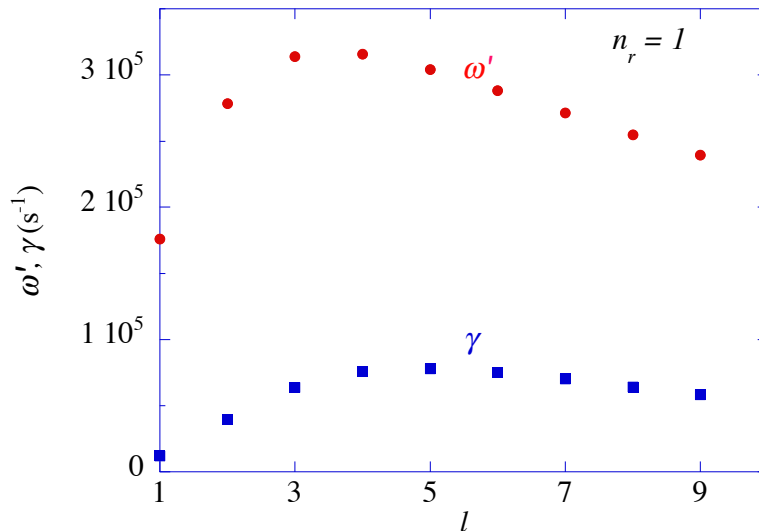


FIGURE 3. Real and imaginary parts of the drift wave frequency for the same plasma as in Fig. 2 versus azimuthal mode number ℓ , for radial mode number $n_r = 1$. Here, $\omega_r = \omega - \ell\omega_i(r)$ is plotted at $r = 0.5$ cm, so as to subtract out the large rotational Doppler shift in the mode frequency. At $r = 0.5$ cm, $\omega_i(r) = 9.25 \times 10^5 \text{ s}^{-1}$.

thermal equilibrium state shown in Fig. 1. Cooling the plasma back to 300K would return the ions to the periphery, allowing a repetition of the experiment in a fully-confined plasma.

In conclusion, we have discussed how centrifugal force in multispecies nonneutral plasma can affect the equilibrium and dynamics, focusing on the phenomenon of centrifugal separation. While collisional centrifugal separation rates are fairly slow in many cases, these rates can be greatly enhanced by the diocotron and drift wave instabilities discussed here.

ACKNOWLEDGMENTS

This work was supported by National Science Foundation Grant No. PHY0903877 and Department of Energy Grant DE-SC0002451.

REFERENCES

1. D. J. Larson, J. C. Bergquist, J. J. Bollinger, Wayne M. Itano, and D. J. Wineland, Phys. Rev. Lett. **57**, 70 (1986).
2. B. M. Jelenkovic, A. S. Newbury, J. J. Bollinger, W. M. Itano, and T. B. Mitchell, Phys. Rev. A **67**, 063406 (2003).
3. G. B. Andresen *et al.* (ALPHA Collaboration), Phys. Rev. Lett. **106**, 145001 (2011).
4. E. Sarid, F. Anderegg and C. F. Driscoll, Phys. Plasmas **2**, 2895 (1995).
5. M. Affolter, F. Anderegg, C. F. Driscoll, and D. H. E. Dubin, "Cyclotron Resonances in a Non-Neutral Multispecies Ion Plasma," this proceedings (2012).
6. A. .A. Kabantsev, private communication.

7. D. H. E. Dubin, Phys. Plasmas **17**, 112115 (2010).
8. D. H. E. Dubin and T. M. O'Neil, Rev. Mod. Phys. **71**, 87 (1999).
9. T. M. O'Neil, Phys. Fluids **24**, 1477 (1981).
10. D. H. E. Dubin, in progress.
11. D. H. E. Dubin, Phys. Rev. Lett. **79**, 2678 (1997).